Desalination and Water Treatment
www.deswater.com

doi:10.5004/dwt.2017.20980

93 (2017) 30–39
October

Removal of hardness from groundwater using two nanofiltration membranes: experimental study and modeling

Mohamed Igouzal[a], Fatima El Azhar[b], Mahmoud Hafsi[c], Mohamed Taky[b], Azzedine Elmidaoui[b,*]

[a]*Interdisciplinary Laboratory for Natural Resources and Environment, Faculty of Sciences, Ibn Tofail University*
[b]*Laboratory of Separation Processes, Department of Chemistry, Faculty of Sciences, Ibn Tofail University , P.O. Box 1246, Kenitra 14000 – Morocco, elmidaouiazzedine@hotmail.com*
[c]*International Institute for Water and Sanitation, National office of Electricity and Potable water (ONEE-IEA), Rabat, Morocco*

Received 3 August 2016; Accepted 25 May 2017

ABSTRACT

Water hardness causes potentially costly nuisance problems in homes and in industry, such as disabling washing, formation of tartar carbonate and magnesium hydroxide in the pipe network of hot water. In this work, the ability of two commercial nanofiltration membranes (NF90, NF270) to remove hardness from the Maâmora groundwater (North of Morocco) was studied. Experiments were carried out in the pressure range of 5–40 bar and for different total hardness (TH) of the feed water. The effects of the trans-membrane pressure on the permeate flux and retention rate were investigated for each membrane. The results show that the nanofiltration membranes are capable of retaining the total hardness present in groundwater. Experiment results were correlated and analysed using Spiegler–Kedem model. Model parameters (the reflection coefficients and the solute permeability) have been determined for the two membranes using an adequate mathematical optimization procedure (Levenberg-Marquardt´s algorithm: LMA). Model predictions of Ca^{2+} and Mg^{2+} rejection were used to calculate rejection for Total Hardness. The modeling results were in good agreement with the experimental data for both NF90 and NF270 membrane. The correlation coefficient was greater than 0.9 in all cases. Also, statistical analysis of residual errors based on the root mean square error (RMSE), the normalized root mean square error (NRMSE) and the Nash-sutcliffe efficiency (NSE) coefficient demonstrates the good performance of the model and the optimization procedure. Results of this study are of great importance for local managers since waters of Maâmora groundwater are locally used in many areas and are part of several water management plans.

Keywords: Nanofiltration; Total hardeness; Spiegler–Kedem model; Maâmora groundwater

I. Introduction

Master plans for water resource development in Morocco foresee a shortage in potable water from conventional resources by the year 2030. The impact of the Rainwater variability and the climate change will make the situation more problematic. Since 1980s, Morocco has anticipated this problem and resorted to the desalination of brackish water by membrane techniques to supply traditionally deficient regions with good quality water. In order to choose reliable technology that could be adapted to relatively large capacities and specifications (energy costs), ONEE (National Office of Water and Electricity) had formed personnel and many desalination plants were build. The largest desalination plant currently in operation is that of Laayoune town seawater reverse osmosis plant (south of Morocco) [1–3]. Other similar projects also apply reverse osmosis (RO) process rather than other techniques like nanofiltration (Table 1).

In Morocco, nanofiltration is widely studied at laboratory and pilot scales [4,5]. However, its implementation on an industrial scale is not yet well exploited. The only exam-

*Corresponding author.

Table 1
Production of current desalination plants in Morocco

Process	City	Capacity (m^3/d)
Desalination	Laâyoune	25920
	Boujdour	9504
	Akhéfnir	864
	Sidi EL Ghazi	89.856
	Roc Chicco	30.24
Demineralisation	Tarfaya	864
	Daoura	233.28
	Tan-Tan	3456
	EL ouatia	8640
	Tagounite	432
Demineralisation of fresh water	Khénifra	9849.6
Desulfurisation-	Dakhla station 1	9504
Nitrification-demineralisation	Dakhla station 2	17280
Total (m^3/d)		86667

ple of the implementation of this technique is that of the groundwater demineralisation plant in the commune of Sidi Taibi (Near Kénitra Town). The feed water of this plant is pumped from Maâmora aquifer. The water is slightly brackish, with nitrate levels that moderately exceeds the water quality international standards [6]. The station is installed in a high school and works with renewable energy combining solar and wind resources to provide drinking water to students. This station has been in operation since 2014 and, except the problem of the nanofiltration membrane fouling, this technique is entirely satisfactory. In this study waters treated by NF comes from the same water table (The Maâmora groundwater) and hardness elimination was targeted.

Water hardness is primarily the amount of calcium and magnesium, and to a lesser extent, iron in the water. It is measured by adding up the concentrations of calcium, magnesium and converting this value to an equivalent concentration of calcium carbonate ($CaCO_3$). Hard water is mainly an aesthetic concern because of the unpleasant taste that a high concentration of calcium and other ions give to water. It also reduces the ability of soap to produce a lather, and causes scale formation in pipes and on plumbing fixtures. Soft water can cause pipe corrosion and may increase the solubility of heavy metals such as copper, zinc, lead and cadmium in water [7].

In many regions groundwater tends to be harder than surface water. Water hardness in most groundwater is naturally occurring from weathering of limestone, sedimentary rock and calcium bearing minerals. Hardness can also occur locally in groundwater from chemical and mining industry effluent or excessive application of lime to the soil in agricultural areas. In some agricultural areas where lime and fertilizers are applied to the land, excessive hardness may indicate the presence of other chemicals such as nitrate. Therefore, removal of these ions from waters has been an area of substantial technological interest in all over the world [8].

The traditional processes for water softening include lime-soda and ion exchange processes [9]. Recent works use an application of kenaf fibers (Hibiscus cannabinus L.) in water hardness reduction [10].

Membrane softening is becoming an alternative to these processes. Nanofiltration process with charged membranes can be used for hardness reduction. It has attracted increasing attention over the recent years due to its remarkable ability to selectively reject different dissolved ions, even these with low molecular weight. In addition, the NF membranes can provide high water flux at low operating cost and low energy consumption [11,12].

The rejection of ions by NF membranes is the consequence of the combination of steric and electric interactions. NF membranes reject multivalent ions more efficiently than monovalent ions which are partly rejected. The concentration difference between feed and permeate is smaller than for a complete rejection (reverse osmosis processes). This is an advantage for NF because in this casethe osmotic pressures are lower compared to reverse osmosis, so that lower pressure need to be applied and the energy consumption is proportionally lower [3,13,14].

Nanofiltration is now widely used in various fields such as for water and wastewater treatment in order to remove suspended solids and reduce the content of organic and inorganic matters. Many authors have reported the application of NF to highly reduce TDS, nitrates, hardness, cyanides, fluorides, arsenic, heavy metals, color and organic compounds, e.g., totalorganic carbon (TOC), biological oxygen demand (BOD), chemical oxygen demand (COD), and pesticides, besides the elimination of bacteria, viruses, turbidity and TSS from surfacewater, groundwater and seawater [5].

Schaep et al. [15] studied hardness reduction in groundwater achieved by nanofiltration membranes. They studied three commercial nanofiltration membranes and concluded that the performance of the UTC20 nanofiltration membrane for reducing hardness was better than that of the NF70 and UTC60 nanofiltration membranes.

Gorenflo et al. [16] examined the nanofiltration of German groundwater with high hardness. They used NF200B nanofiltration with 5.5 bar transmembrane pressure. The rejection of Ca^{2+} and Mg^{2+} was high (~74% and >86%, respectively).

Ghizellaoui et al. [17] studied the use of nanofiltration for partial softening of very hard water of Hamma underground water, which provides drinking water for Constantine City (Algeria). Two techniques were used to obtain a partial softening based on applying weak pressure (0.5, 1, 2 bar) or relatively high pressure (4–16 bar) to feed water. Retention reached 50% for Ca^{2+} and 40% for HCO_3^- at relatively high pressures and 34% for Ca^{2+} and 30% for HCO_3^- at low pressures.

Galanakis et al. [18] performed nanofiltration of brackish groundwater by using a poly-piperazine membrane. They used cross flow nanofiltration module and low transmembrane pressure (6–10 bar). Their results showed that this nanofiltration membrane could remove 70–76% of hardness.

Gilron et al. [19] studied the transport of 1500 ppm and 15,000 ppm NaCl in commercial polypiperazine nanofiltra-

tion membrane. According to the manufacturer, the rejection of NaCl by this membrane is 70%. The feed flux varied approximately between 20 L $m^{-2} h^{-1}$ to 100 L $m^{-2} h^{-1}$.

Recently, El Azhar et al. [20] have used two nanofiltration membranes (NF90 and NF270) in hardness removal from groundwater. They studied the effects of pressure and flow rate on the nanofiltration performance at various concentrations of TH ($CaCl_2$, $MgCl_2$). Their results showed that nanofiltration separation could remove from 97 to 98% of hardness with NF90 and from 47% to 70% with NF270.

On other hand, numerous phenomenological and mechanistic models have been proposed to describe solute and solvent transport through porous and dense membranes [21]. For dense membranes, most popular is the "solution-diffusion" model, in which solutes dissolve at the membrane interface and then diffuse through the membrane along the concentration gradient. In this model, separation between different solutes results from dissimilarities in the amount of mass that dissolves per membrane volume and/or the rate at which it diffuses through the membrane [22]. Pore-flow models also exist, in which different solutes are separated by size, frictional resistances, and/or charge. In addition to the solution-diffusion and pore-flow models, the Kedem–Katchalsky and Spiegler–Kedem models employ irreversible thermodynamic arguments to derive solute and solvent transport equations while treating the membrane as a "black box" [23,24].

Recently, solute/solvent–membrane affinity has also been taken into account in the convection-diffusion-affinity model [25]. Finally, mixed-matrix membranes introduce new complexities into membrane transport where multiple phases potentially containing different characteristic pore size, solubility, and diffusivity are present within a single membrane.

Spiegler–Kedem model correlates transport with mechanical and osmotic pressure gradients. It assumes that the membrane near to equilibrium and the system can be divided into small sub-systems in which local equilibrium exists. Fluxes are derived from phenomenological thermodynamic relationships. However, this model do not provides insights into mechanistic transport. Koyuncu and Yazgan [26] found that this model was able to fit well their experimental data (rejection versus permeate flux) for different salt mixtures using TFC-S NF membrane. They concluded that the reflection coefficient is constant for each anions and cations in the salt mixture whereas the permeability coefficient was varied according to the type of the salt ions. Nevertheless, different conclusion has been obtained by other authors [27–29] for the filtration of single salts showing that both model parameters have changed and were dependent on the type of the filtered salt. Other authors proposed an extended Spiegler-Kedem (ESK) model by incorporating solute-solute interactions in the nanofiltration of multiple solutes systems [30].

Chaudry [31] used the Spiegler-Kedem model to calculate the percentage of diffusive and convective fluxes in symmetric lab-made cellulose acetate membranes. He found that 63% of the total NaCl flux is attributed to diffusion transport and that the rest of about 37% is due to the salt convective flux.

The Spiegler-Kedem model was also used by Gilron et al. [10] to calculate the relative distribution of the salt flux through the membrane. The authors found that at least half of the salt flux is due to convective coupling, with the diffusive flux decreasing with the increase in the feed flux.

Models based on irreversible thermodynamics approach are easiest to use, especially Spiegler-Kedem model which requires only two parameters for its application. This model is recommended for studies representing first attempts of modeling membranes processes. In addition, it is methodologically correct to start with the simplest description of the phenomena under study and to evaluate the limits of this approximation before investigating more complications. For all these reasons the use of S-K model is adequate in our case study.

Maâmoura groundwater provides drinking water for many Moroccancities like Kenitra and the capital Rabat. Previous works revealed that Maâmoura groundwater is further characterized by a particularly high level of total hardness and that rock formations containing divalent metals (Mg^{2+}, Ca^{2+}) are responsible for this excessive hardness [32]. The object of this paper is to study the ability of a nanofiltration membranes (NF90, NF270) to remove hardness from groundwater of Maâmoura region (North of Morocco).The influence of different operational conditions (pressure, feed concentration) on total hardness removal is investigated. The viability of using the Spiegler–Kedem model to predict the rejection of Ca^{2+} and Mg^{2+} with the different membranes studied is examined.

2. Theoretical background: Spiegler–Kedem model

Membranes performance is measured in terms of salts rejection R (%) and permeate flux, J_v (m/s). For dilute aqueous mixtures consisting of water and a solute, the selectivity of a membrane toward the mixture is usually expressed in terms of the observed solute rejection coefficient. This parameter is a measure of the membrane ability to separate the solute from the feed solution and is defined as:

$$R(\%) = 100\frac{C_f - C_p}{C_f} \tag{1}$$

where C_p and C_f are the solute concentration in the permeate and feed solution, respectively.

The Spiegler-Kedem (SK) model provides a simple framework for description of solute transport in both RO and NF processes. In this model, the membrane is regarded as a "black-box". The SK model considers convective coupling of solute and solvent species.

For the derivation of the SK model, the starting point is the assumption that the water flux (J_v) and the solute flux (J_s) are driven by forces F_v and F_s, respectively. These generalized forces are due to chemical potential gradients across the membrane:

$$J_v = L_{11}F_v + L_{12}F_s \tag{2}$$

$$J_s = L_{21}F_v + L_{22}F_s \tag{3}$$

where L_{ij} are phenomenological coefficients.

The chemical potential gradient is caused by a concentration or pressure gradient. So that the final working equations of the nonlinear SK model are:

$$J_v = L_p \cdot \left(\frac{dP}{dx} - \sigma \frac{d\Pi}{dx} \right) \quad (4)$$

$$J_s = P_s \cdot \frac{dC_s}{dx} + (1-\sigma) \cdot C_s \cdot J_v \quad (5)$$

where J_v (kg/m² s): water flux. J_s (kg/m² s): solute flux. L_p (m/s): solvent permeability constant. (Pa): operation pressure. Π (Pa): osmotic pressure. x (m): distance across the membrane. C_s: solute concentration inside the membrane. P_s (m/s): solute permeability constant. σ: reflection coefficient.

Solvent transport is due to the pressure gradient across the membrane and solute transport is due to the concentration gradient and convective coupling of the volume flow. Solute transport in RO membranes occurs predominantly via diffusion, however, for membranes with larger pores such as NF ones, both the convective and diffusive contributions to the solute flux are important and cannot be ignored [3]. Hence, Eq. (4) shows that the solute flux is the sum of diffusive and convective terms. Solute transport by convection takes place because of an applied pressure gradient across the membrane. A concentration difference on both sides of the membrane causes diffusive transport.

Integration of Eqs. (4) and (5) combined with Eq. (1) and considering the limit conditions of the problem (for $x = 0$, $C_s = C_f$ and for $x = \Delta x$, $C_s = C_p$) lead to Eqs. (6) and (7):

$$R = 1 - \frac{C_p}{C_f} = \frac{\sigma(1-F)}{1-\sigma F} \quad (6)$$

$$F = \exp\left(-\frac{(1-\sigma)J_v}{P_s} \right) \quad (7)$$

where C_f (kg/m³): solute concentration in the feed solution. C_p (kg/m³): solute concentration in the permeate solution. F (dimensionless): a flow parameter. Δx (m): membrane thickness.

The two transport parameters (σ and P_s) are the main parameter of the model. The parameters σ is a measure of the degree of semipermeability of the membrane, i.e. its ability to pass solvent in preference to solute. It characterized the imperfection of the membrane [3] while the parameters P_s is associated to diffusive properties. Concentration dependence of these coefficients is assessed by fitting the data for different feed concentrations. A value of σ = 1 means that the convection solute transport does not take place at all. This is the case for ideal RO membranes where the membranes have no pores available for the convective transport. In an entirely unselective membrane, in which a concentration gradient does not cause volumetric flow at all, σ = 0. For the UF (untrafilration) and NF membranes which have pores, the reflection coefficient will be σ < 1, especially if the solutes are small enough to the entire membrane pores under the convective transport effect [6].

In this study, the model parameters σ and P_s were optimized using the Levenberg-Marquardt´s algorithm (LMA) to fit the experimentally obtained rejection permeation data to the model calculated rejection [33]. The LMA algorithm solves non-linear least-squares problems in mathematics and computing using an iterative minimization technique. The LMA is used in many software applications for solving generic curve-fitting problems. The algorithm combines advantages of the steepest descent method (that is, minimization along the direction of the gradient) with the Newton method (that is, using a quadratic model to speed up the process of finding the minimum of a function). Also, LMA algorithm finds a solution (parameters estimation) even if it starts very far off the final minimum. The calculated coefficients (σ and P_s) are said to represent the values of the transport coefficients for the given feed salt composition. Concentration dependence of these coefficients can be assessed by fitting the data with the LMA algorithm for different feed concentrations.

3. Materials and methods

3.1. Brackish groundwater

The nanofiltration operations were conducted for an underground water of Maâmoura region doped for the three concentrations of TH ($CaCl_2$, $MgCl_2$) for three feed water (FW) having respective hardness of 100 °fH (FW1), 150 °fH (FW2) and 200 °fH (FW3). Table 2 gives the characteristic of the brackish groundwater and the Moroccan standards of drinking water. The total hardness is mainly due to the presence of Ca^{2+} rather than Mg^{2+}.

3.2. Pilot plant

NF experiments were performed on an industrial pilot NF/RO (E3039) provided by the company TIA (Applied Industrial Technologies, France) (Fig. 1). The applied pressure over the membrane can be varied from 5 to 70 bar with manual valves. The operations were designed in a continuous simple pass mode. The pilot is equipped with two identical modules in series. The pressure drop ΔP is about 2 bar. The two spiral wound modules are equipped with two commercial reverse osmosis and nanofiltration membranes. Table 3 gives the characteristics of the used membranes.

Table 2
Characteristic of brackish groundwater

Parameters	FW1	FW2	FW3	Norms
pH	6,70	6,98	6,73	6,50–8,50
Turbidity (NTU)	0,50	0,92	1,02	5
Conductivity (µS/cm)	1793	2200	3050	–
TDS (mg l^{-1})	1344,75	1650	2287,5	500
Total Hardness (°fH)	100	150	200	50
Total Alkalinity (°fH)	26	26	26	–
Ca^{2+} (mg l^{-1})	278,4	339,2	435,2	250
Mg^{2+} (mg l^{-1})	7,68	10,24	17,92	50
Na^{+} (mg l^{-1})	56,40	56,40	56,40	250
K^{+} (mg l^{-1})	1,84	1,84	1,84	–
SO_4^{2+} (mg l^{-1})	60	60	60	400
Cl^{-} (mg l^{-1})	541,38	665,63	1020,63	250
NO_3^{-} (mg.l^{-1})	41	41	41	50

3.3. Statistical analysis

In this study, a statistical analysis of residual errors based on the root mean square error (RMSE), the normalized root mean square error (NRMSE) and the Nash-Sutcliffe efficiency (NSE) coefficient was performed.

$$RMSE = \sqrt{\left[\frac{\sum_{i=1}^{n}\left(x_{meas,i} - x_{pred,i}\right)^2}{N}\right]} \quad (8)$$

where $x_{meas,i}$: measured retention rate, $x_{pred,i}$: calculated retention rate.

The RMSE is the distance, on average, of a data point from the fitted line, measured along a vertical line. It is directly interpretable in terms of measurement units, and so is a better measure of goodness of fit than the correlation coefficient.

$$NRMSE = \frac{RMSE}{\bar{x}_{meas}} \quad (9)$$

where $\bar{x}_{meas}$: mean measured retention rate.

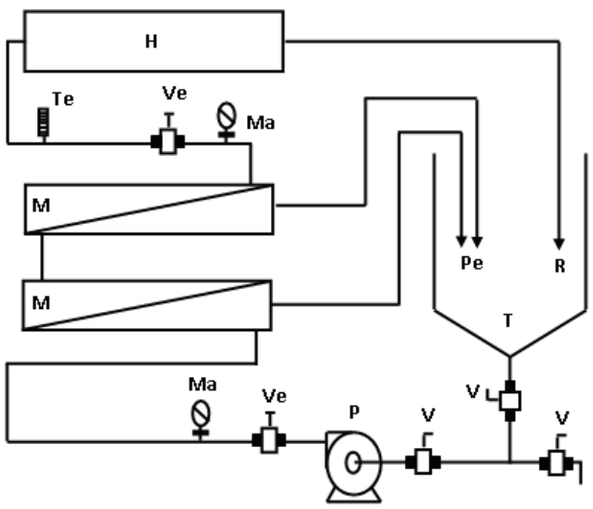

Fig. 1. Diagram of the NF/RO pilot plant.
T : tank; P : feed pump; Ve : pressure regulation valves; V : drain valves; M : NF/RO module; Pe : Permeate recirculation; R : Retentate recirculation; H : Heat exchanger; Ma : Pressure sensor; Te : Temperature sensor.

The normalized root mean square error (NRMSE) represents a non-dimensional form of the RMSE. A lower value of NRMSE indicates less residual variance.

$$NSE = 1 - \left[\frac{\sum_{(i=1)}^{n}\left(x_{meas,i} - x_{pred,i}\right)^2}{\sum_{(i=1)}^{n}\left(x_{meas,i} - \bar{x}_{meas}\right)^2}\right] \quad (10)$$

The Nash-Sutcliffe Efficiency (NSE) is a normalized statistic that determines the relative magnitude of the residual variance (noise) compared to the measured data variance (information). It informs on how well the plot of observed versus simulated data fits the 1:1 line.

3.4. Total Hadress rejection calmculation

TH retention is calculated based on Ca^{2+} and Mg^{2+} retentions as follows:

$$TH = \frac{\left[Ca^{2+}\right]10^3}{4} + \frac{\left[Mg^{2+}\right]10^3}{2.43} \quad (11)$$

where $[Ca^{2+}]$: Ca^{2+} concentration and $[Mg^{2+}]$: Mg^{2+} concentration

$$TH_f = \frac{\left[Ca^{2+}\right]_f 10^3}{4} + \frac{\left[Mg^{2+}\right]_f 10^3}{2.43} \quad (12)$$

TH_f, $[Ca^{2+}]_f$, $[Mg^{2+}]_f$: concentration of TH, Ca^{2+} and Mg^{2+} in feed water

$$TH_p = \frac{\left[Ca^{2+}\right]_p 10^3}{4} + \frac{\left[Mg^{2+}\right]_p 10^3}{2.43} \quad (13)$$

TH_p, $[Ca^{2+}]_p$, $[Mg^{2+}]_p$: concentration of TH, Ca^{2+} and Mg^{2+} in permeat water.

TH retention is given by:

$$R_{TH} = 1 - \frac{TH_p}{TH_f} = 1 - \frac{\frac{\left[Ca^{2+}\right]_p 10^3}{4} + \frac{\left[Mg^{2+}\right]_p 10^3}{2.43}}{\frac{\left[Ca^{2+}\right]_f 10^3}{4} + \frac{\left[Mg^{2+}\right]_f 10^3}{2.43}} \quad (14)$$

The Ca^{2+} retention is given by:

$$R_{Ca^{2+}} = 1 - \frac{\left[Ca^{2+}\right]_p}{\left[Ca^{2+}\right]_f} \quad and \quad \left[Ca^{2+}\right]_p = \left(1 - R_{Ca^{2+}}\right)\left[Ca^{2+}\right]_f \quad (15)$$

The Mg^{2+} retention is given by:

$$R_{Mg^{2+}} = 1 - \frac{\left[Mg^{2+}\right]_p}{\left[Mg^{2+}\right]_f} \quad and \quad \left[Mg^{2+}\right]_p = \left(1 - R_{Mg^{2+}}\right)\left[Mg^{2+}\right]_f \quad (16)$$

Table 3
Characteristics of the membranes used

Membrane	Maximum pressure supported	pH tolerated during treatment	Maximum temperature	Maximum permissible concentration of free chlorine
NF90 40*40	40 bar	3–10	45°C	0,1 ppm
NF270 40*40	40 bar	3–10	45°C	0,1 ppm

$$R_{TH} = 1 - \frac{\frac{\left(1 - R_{Ca^{2+}}\right)\left[Ca^{2+}\right]_f 10^3}{4} + \frac{\left(1 - R_{Mg^{2+}}\right)\left[Mg^{2+}\right]_f 10^3}{2.43}}{\frac{\left[Ca^{2+}\right]_f 10^3}{4} + \frac{\left[Mg^{2+}\right]_f 10^3}{2.43}} \quad (17)$$

4. Results and discussion

4.1. Effect of pressure

The experiments were carried out in simple pass configuration. The imposed pressures were: 10, 25 and 40 bar for NF90 and 6, 10, and 25 bar for NF270 following the manufacturer instructions (Table 3). The influence of the pressure on the permeate flux for each feed water shows that the volumetric permeate flux increases linearly with the pressure. The slopes of the curves are equal to the hydraulic permeability of the respective membranes. The permeate flux obtained by the NF270 is higher than the NF90 membrane. This can be attributed to the nature the NF270 membrane which has more opened pores compared to the NF90 membrane.

4.2. Effect of permeate flux on permeate rejection: application of Spiegler–Kedem model

The experimental data of rejection versus permeate flux for all investigated feed waters and membranes (NF270 and NF90) are plotted in Figs. 2 and 3. Highest rejections are obtained for the NF90 membranes as a result of their impermeable structure which has properties close to reverse osmosis (RO) membranes. NF270 membrane has relatively medium rejection. NF selectivity is influenced by chemical phenomena, pore size and electric charge effects in addition to operation conditions. Also, increasing permeate flux lead

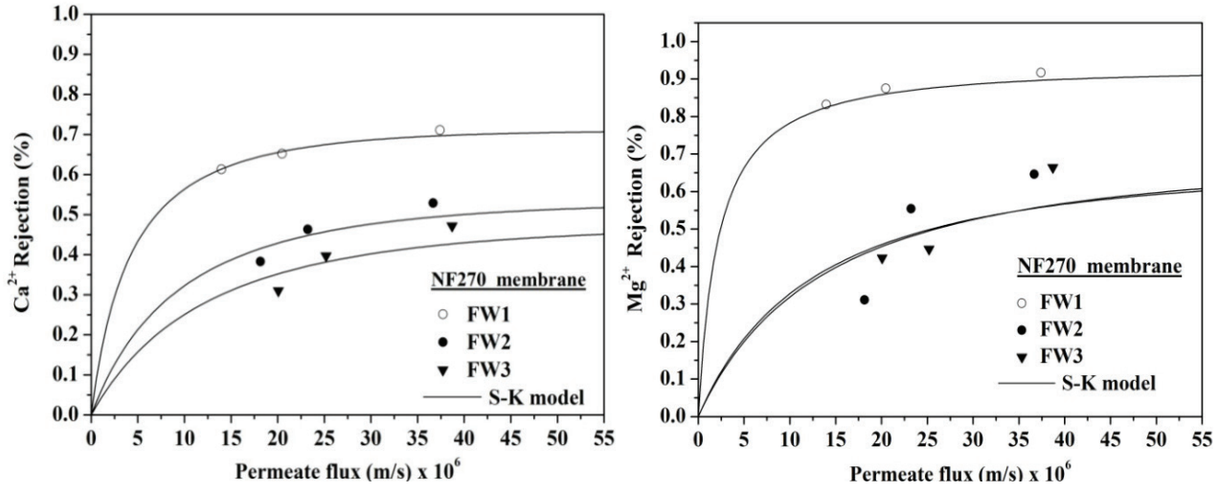

Fig. 2. Effect of permeate flux on rejection of Ca^{2+} and Mg^{2+} using NF270 membrane at various feed water hardness.

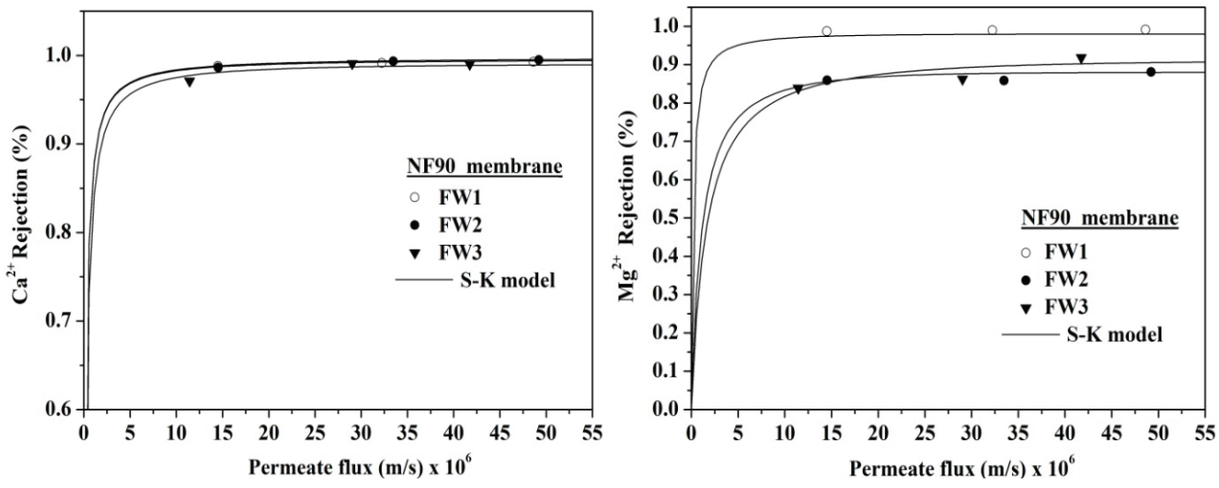

Fig. 3. Effect of permeate flux on rejection of Ca^{2+} and Mg^{2+} using NF90 membrane at various feed water hardness.

to a significant increase in Ca^{2+} and Mg^{2+} rejection, especially for NF270 membrane. This can be explained by the influence of the pressure on the permeate flux as cited above. In other hand, the effect of feed concentration (hardness) on rejection is depicted in Figs. 2 and 3. For NF270, rejection of Mg^{2+} and Ca^{2+} decreases with increasing feed hardness concentration. For NF90 no significant effect of feed concentration on rejection is observed, especially for Ca^{2+}.

The experimental data were fitted on the basis of Spiegler–Kedem model using optimal values of the reflection coefficient (σ) and the solute permeability (P_s) calculated with the LMA algorithm. The rejection rate predicted by the Spiegler–Kedem model is plotted in solid lines in Figs. 2 and 3, for both membranes (NF270 and NF90) and for various concentrations of TH, to provide comparison with measurements. The modeling results show a good fit for the rejection values for each feed water and for all membranes used.

Table 4 summarizes the phenomenological parameters σ and P_s obtained. The values of P_s and σ are dependent on the type of the membrane and on feed water concentration. High values of σ are attributed to NF90 where transport is dominated by diffusion more than convection. Also, for NF270 the coefficient σ decreases so much with increasing feed water hardness, while it still approximately unchanged for NF90 membrane.

Table 4
Parameters σ and P_s estimated by the model

Ca^{2+}				
Membranes	NF270		NF90	
Model parameters	σ	P_s (m/s)	σ	P (m/s)
FW1 (TH = 80 °fH)	0.71	3.87E-06	0.995	1.500E-7
FW2 (TH = 100 °fH)	0.53	8.58E-06	0.997	1.500E-7
FW3 (TH = 150 °fH)	0.47	1.12E-05	0.99	2.00E-7
Mg^{2+}				
Membranes	NF270		NF90	
Model parameters	σ	P_s (m/s)	σ	P (m/s)
FW1 (TH = 80 °fH)	0.99	2E-7	0.91	1.95E-06
FW2 (TH = 100 °fH)	0.65	1.15E-05	0.88	1.05E-06
FW3 (TH = 150 °fH)	0.67	1.26E-05	0.91	1.55E-06

Another way to examine model performance is to plot experimental rejection against predicted rejection (S-K model). In all cases, calculated and experimental rejection are very close, as shown by the good approximation to the diagonal (Figs. 4 and 5). The correlation coefficients are equal to 0.95 (Ca^{2+}) and 0.90 (Mg^{2+}) for NF270 and 0.88 (Ca^{2+}) and 0.94 (Mg^{2+}) for NF90.

4.3. Application of Spiegler–Kedem model to total hardness rejection

Model predictons of Ca^{2+} and Mg^{2+} rejection were used to calculate rejection for Total Hardness. TH rejection versus permeate flux for all investigated feed waters and membranes (NF270 and NF90) are plotted in Fig. 6.

High TH rejections are obtained for the NF90 membrane as a result of its impermeable structure which has properties close to reverse osmosis (RO) membranes. NF270 membrane has relatively medium rejection. Also, increasing permeate flux lead to a significant increase of TH rejection, especially for NF270 membrane. In other hand, the effect of feed concentration (hardness) on rejection is depicted in Fig. 6. For NF270, rejection of TH decreases with increasing feed hardness concentration. For NF90 no significant effect of feed concentration on rejection is observed.

On other hand, Fig. 6 shows a good agreement between the experimental and predicted TH rejection.

4.4. Statistical analysis and model performance tests for total hardness

Another way to examine model performance is to plot experimental rejection against predicted rejection. Fig. 7

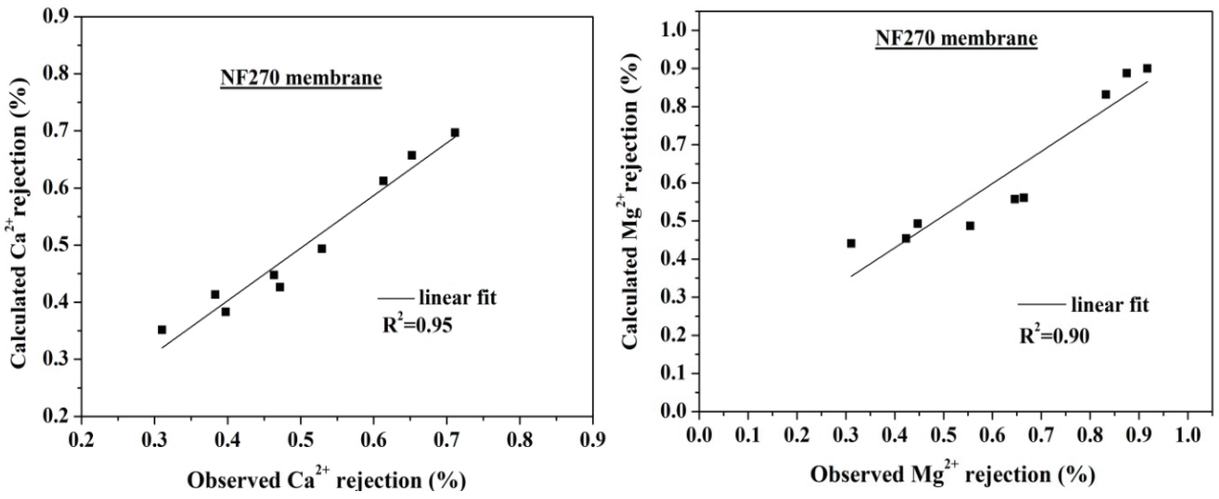

Fig. 4. Parity plots between calculated and measured rejection rates of Ca^{2+} and Mg^{2+} for NF270.

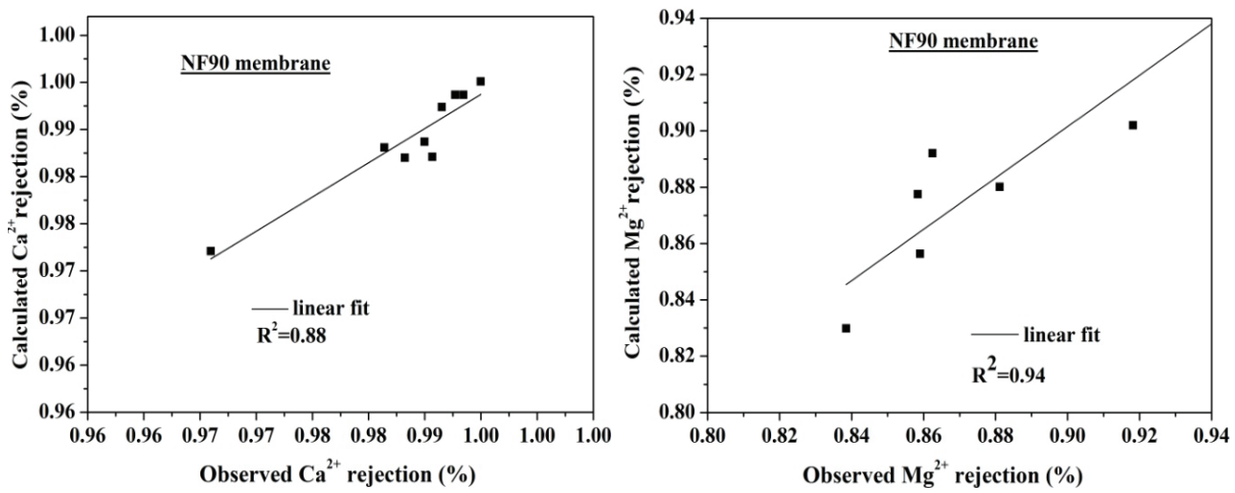

Fig. 5. Parity plots between calculated and measured rejection rates of Ca^{2+} and Mg^{2+} for NF90.

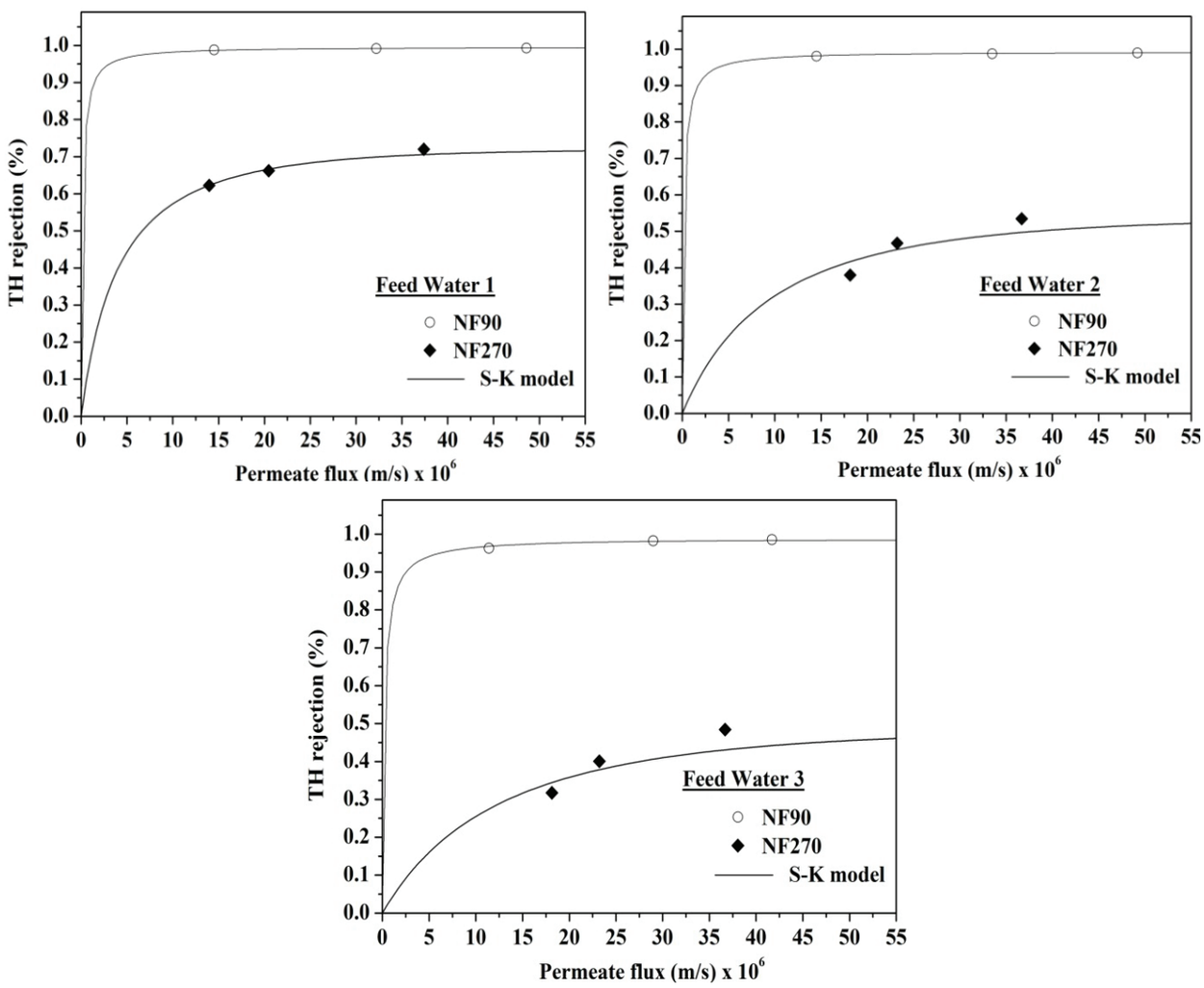

Fig. 6. Effect of permeate flux on rejection of TH for NF270 and NF90 membranes for various feed water.

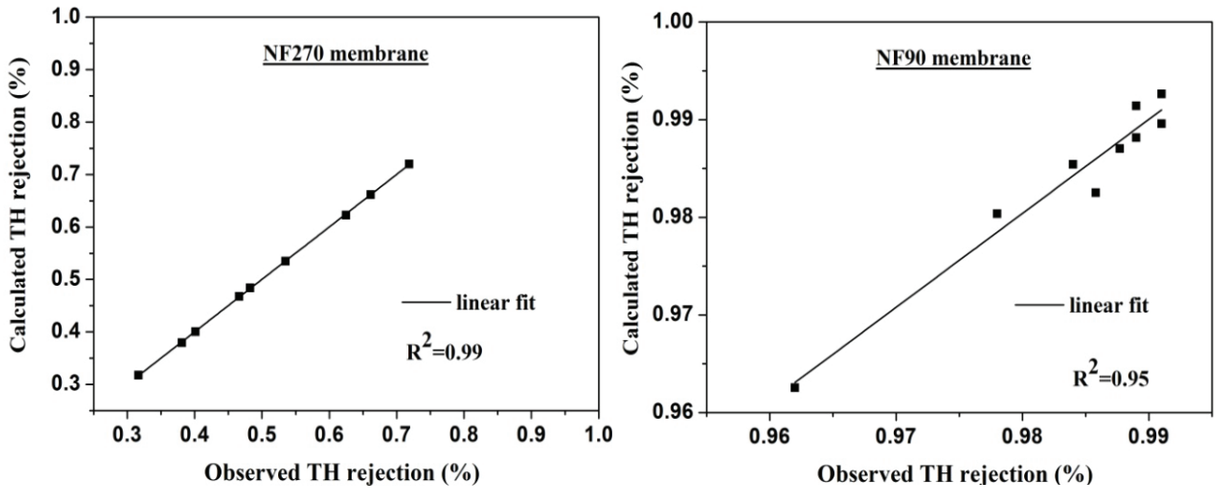

Fig. 7. Parity plots between calculated and observed TH rejection using NF270 and NF90 membranes.

Table 5
Results of the statistical analysis

Membrane	RMSE (%)	NRMSE (–)	NSE (–)
NF90	0,027	0,032	0,95
NF270	0,034	0,050	0,99

shows parity plots between calculated and measured total hardness rejection, using data for the three feed waters tests. Calculated and experimental TH rejection are very close, as shown by the good approximation to the diagonal. The correlation coefficients are superior to 0.95 which show the perfect fit by the model.

Also, Table 5 shows the results of the statistical analysis as described in material and methods section. The RMES coefficient obtained have a small value, the NRMSE function is small than unity and the NSE coefficient is very near to 1. This result demonstrates the good performance of the model and the optimization procedure.

5. Conclusion

Nanofiltration is well studied worldwide in the case of synthetic water, but in the case of natural water results of nanofiltration application differ according to water constitution due to the numerous interactions between constituents. Data for membrane performances correspond to their use with synthetic water and for their use as new membranes. Due to aging (time and type of use), the membranes lose their performance as demonstrated by many authors. Hence, in each studied case, experimentation on pilot can bring a scientific novelty.

In this work, separation performance (rejection and flux) of groundwater of Maâmoura region (North of Morocco) with different total hardness was investigated using two nanofiltration commercial membranes (NF270 and NF90).The Spiegler-Kedem model was used to fit the experimental data of rejection versus the permeate flux. Results showed a good agreement between model calculations and experimental data for the two membranes and feed water hardness. Optimal values of model parameters, σ and P_s, were estimated using an adequate mathematical optimization procedure (Levenberg-Marquardt´s algorithm) and are in concordance with membranes proprieties and vary depending on feed TH as can be expected. The correlation coefficient obtained between model calculations and measurements was greater than 0.88 in all cases. This simple model successfully used here for modelling Total Hardness remove by NF can be a helpful tool for designing possible practical applications. Results of this study are of great importance for local managers since water used is a ground water from the Maâmora zone and is locally solicited in many areas. Also, authors of the present research have been working closely together, for many years, with ONEE's engineers. Some research results of this long term collaboration have been exploited in the ONEE drinking water production plants. The present work represents a continuity of this fruitful collaboration. The novelty of the work is that the water treated and membranes used form a special case study. Also, the study represents a first attempt to apply mathematical modeling on Maâmora groundwater using nanofiltration data.

Symbols

C_f (kg/m^3) — Solute concentration in the feed stream
C_m (kg/m^3) — Solute concentration in the membrane
C_p (kg/m^3) — Solute concentration in the permeate stream
R^2 — Correlation coefficient
F — Dimensionless parameter of SKK model
FW — Feed water
J_v (m^3/m^2 s) — Permeate flux
J_s (kg/m^2 s) — Solute flux
J_w (kg/m^2 s) — Water flux
L_p (m/s) — Solvent permeability constant

NSE — Nash-Sutcliffe efficiency
NRMSE — Normalized Root Mean Square Error
P (Pa) — Operation pressure
P_s (m/s) — Solute permeability constant
R (%) — Membrane rejection
RMSE — Root Mean Square Error
TH — Total Hardness
T (°C) — Temperature
σ — Reflection coefficient
x (m) — Distance across the membrane
ΔP (Pa) — Hydraulic pressure applied across the membrane
Δx (m) — Membrane thikness
$\Delta\Pi$ (Pa) — Difference in the osmotic pressure of the solutions on the feed and permeate side of the membrane.

References

[1] H. Zidouri, Desalination of Morocco and presentation of design and operation of the Laayoune seawater reverse osmosis plant, Desalination, 131 (2000) 137–145

[2] A. Boughriba, Experiences and prospects of desalination in Morocco, Course on desalination of sea water and brackish waters (in French), Organized by MEDRC, ENIM, Rabat, Morocco. 2004.

[3] H. Dach, Comparison of the operations of nanofiltration and reverse osmosis for the selective desalination of brackish water: of the scale of the laboratory to the industrial pilot, Thesis, Université of Angers, France. (2008).

[4] M. Pontié, H. Dach, J. Leparc, M. Hafsi, A. Lhassani, Novel approach combining physico-chemical characterizations and mass transfer modelling of nanofiltration and low pressure reverse osmosis membranes for brackish water desalination intensification, Desalination, 221 (2008) 174–191.

[5] K. Khaless, A, Kossir, Process for purifying phosphoric acid by nanofiltration, WO 2013133684A1, OCP Group, Morocco. 2013.

[6] A. El Midaoui, The issue of energy and water in Morocco and the role renewable energies and unconventional water resources. Monaco Internationnal Forum on Water, October 7, Monaco, France. 2013.

[7] G. Devikavathi, C. Muralidharan, An approach towards redefining water quality parameters for leather industry. Part 1. Effect of hardness and chlorides in water, Desal. Water Treat., 21 (2010) 53–59.

[8] L. Fu, J. Wang, Y. Su, Removal of low concentrations of hardness ions from aqueous solutions using electrodeionization process, Sep. Purif. Technol., 68 (2009) 390–396.

[9] Wu Daoji, Tie Zhongyong, Wang Lin, Tan Fengxun, Han Qingxiang, Yu Xiaobin, Process design of water treatment plant on groundwater with high hardness in Yucheng, Desal. Water Treat., 51 (2013) 2715–3720.

[10] E. Gharehchahi, A. Hossein Mahvi, S.M. Taghavi Shahri, R. Davani, Possibility of application of kenaf fibers (Hibiscus cannabinus L.) in water hardness reduction, Desal. Water Treat., 52 (2014) 31–33.

[11] A.A. Izadpanah, A. Javidnia The ability of a nanofiltration membrane to remove hardness and ions from diluted seawater, Water, 4 (2012) 283–294.

[12] M. Tahaikt, R. El Habbani, A. Ait Haddou, I. Achary, Z. Amor, M. Taky, A. Alami, A. Boughriba, M. Hafsi, A. Elmidaoui, Fluoride removal from groundwater by nanofiltration, Desalination, 212 (2007) 46–53.

[13] F. Elazhar, M. Tahaikt, A. Achatei, F. Elmidaoui, M. Taky, F. El Hannouni, I. Laaziz, S. Jariri, M. El Amrani, A. Elmidaoui, Economical evaluation of the fluoride removal by nanofiltration, Desalination, 249 (2009) 154–157.

[14] M. Tahaikta, A. Ait Haddou, R. El Habbani, Z. Amor, F. Elhannouni, M. Taky, M. Kharif, A. Boughriba, M. Hafsi, A. Elmidaoui, Comparison of the performances of three commercial membranes in fluoride removal by nanofiltration. Continuous operations, Desalination, 225 (2008) 209–219.

[15] J. Schaep, B.van der Bruggen, S. Uytterhoeven, R. Croux, C. Vandecasteele, D. Wilms, E. van Houtte, F. Vanlerberghe, Removal of hardness from groundwater by nanofiltration, Desalination, 119 (1998) 295–302.

[16] A. Gorenflo, D. Velazquez-Padron, F.H. Frimmel, Nanofiltration of a German groundwater of high hardness and NOM content: Performance and coast, Desalination, 151 (2002) 253–265.

[17] S. Ghizellaoui, A. Chibani, S. Chizellaoui Use of nonofiltration for partial softening of very hard water, Desalination, 179 (2005) 315–322.

[18] C.M. Galanakis, G. Fountoulis, V. Gekas Nanofiltration of brackish groundwater by using a polypiperazine membrane, Desalination, 286 (2012) 277–284.

[19] J. Gilron, N. Gara, O. Kedem, Experimental analysis of negative salt rejection in nanofiltration membranes, J. Membr. Sci., 185 (2001) 223–236.

[20] F. Elazhar, R. EL Habbani, M. Elazhar, M. Hafsi, A. Elmidaoui, Comparison of the performances of two commercial membranes in hardness removal from underground water using Nanofiltration membranes, Int. J. Adv. Chem., 1(2) (2013), 21–30.

[21] J. Wang, D.S. Dlamini, A.K. Mishra, M.T. Pendergast, M.C.Y. Wong, B.B. Mamba, V. Freger, A.R.D. Verliefde, E.M.V. Hoek, A critical review of transport through osmotic membranes, J. Membr. Sci., 454 (2014) 516–537.

[22] M.F. San Román, E. Bringas, R. Ibañez, I. Ortiz, Liquid membrane technology: fundamentals and review of its applications, J. Chem. Technol. Biotechnol., (2010) 852–10.

[23] G. Suchanek, Mechanistic equations for membrane transport of multicomponent solutions, Gen. Physiol. Biophys., 25 (2006) 53–63.

[24] V. Nikonenko, V. Zabolotsky, C. Larchet, B. Auclair, G. Pourcelly, Mathematical description of ion transport in membrane systems, Desalination, 147 (2002) 369–374.

[25] A.R.D. Verliefde, E.R. Cornelissen, S.G.J. Heijman, E.M.V. Hoek, G.L. Amy, B.V. Bruggen, J.C. van Dijk, Influence of solute membrane affinity on rejection of uncharged organic solutes by nanofiltration membranes, Environ. Sci. Technol., 43 (2009) 2400–2406.

[26] I. Koyuncu, M. Yzgan, Application of Nanofiltration and reverse osmosismembranes to the salty and polluted surface water, J. Environ. Sci. Health, 36(7) (2001) 1321–1333.

[27] J. Gilron, N. Gara, O. Kedem, Experimental analysis of negative salt rejection in nanofiltration membranes, J. Membr. Sci., 185 (2001) 223–236.

[28] C.K. Diawara, M. Sidy Lô, M. Rumeau, M. Pontie, O. Sarr, A phenomenological mass transfer approach in nanofiltration of halide ions for a selectivedefluorination of brackish drinking water, J. Membr. Sci., 219 (2003) 103–112.

[29] A. Hafiane, D. Lemordant, M. Dhahbi, Removal of hexavalent chromium by nanofiltration, Desalination, 130 (2000) 305–312.

[30] A.L. Ahmad, M.F. Chong, S. Bhatia, Mathematical modeling and simulation of the multiple solutes system for nanofiltration process, J. Membr. Sci., 253 (2005) 103–115.

[31] M.A. Chaudry, Water and ions transport mechanism in hyperfiltration with symmetric cellulose acetate membranes, J. Membr. Sci., 5204 (2002) 1–14.

[32] I. Kherrati, A. Alemad, M. Sibbari, H. Ettayea, K. Ezziani, Y. Saidi, M. Benchikh, S. Alzwi, H. Chiguer, Z. Zgourdah, A. Bourass, H. Daifi, O. Elrhouat, K. Elkharrim, D. Belghyti, Health risk of Maâmora's groundwater pollution in Morocco, Natural Res., 6 (2015) 290–305.

[33] K. Levenberg, A method for the solution of certain problems in least squares, dans Quart. Appl. Math., 2 (1944) 164–168.